



UNIVERSITY OF LEEDS

This is a repository copy of *Reconstruction of the perfusion coefficient from temperature measurements using the conjugate gradient method*.

White Rose Research Online URL for this paper:
<http://eprints.whiterose.ac.uk/112412/>

Version: Accepted Version

Article:

Cao, K and Lesnic, D (2018) Reconstruction of the perfusion coefficient from temperature measurements using the conjugate gradient method. *International Journal of Computer Mathematics*, 95 (4). pp. 797-814. ISSN 0020-7160

<https://doi.org/10.1080/00207160.2017.1296955>

© 2017 Informa UK Limited, trading as Taylor & Francis Group. This is an Accepted Manuscript of an article published by Taylor & Francis in *International Journal of Computer Mathematics* on the 13th March, 2017, available online:
<http://www.tandfonline.com/10.1080/00207160.2017.1296955>

Reuse

Unless indicated otherwise, fulltext items are protected by copyright with all rights reserved. The copyright exception in section 29 of the Copyright, Designs and Patents Act 1988 allows the making of a single copy solely for the purpose of non-commercial research or private study within the limits of fair dealing. The publisher or other rights-holder may allow further reproduction and re-use of this version - refer to the White Rose Research Online record for this item. Where records identify the publisher as the copyright holder, users can verify any specific terms of use on the publisher's website.

Takedown

If you consider content in White Rose Research Online to be in breach of UK law, please notify us by emailing eprints@whiterose.ac.uk including the URL of the record and the reason for the withdrawal request.



eprints@whiterose.ac.uk
<https://eprints.whiterose.ac.uk/>

Reconstruction of the perfusion coefficient from temperature measurements using the conjugate gradient method

K. Cao, D. Lesnic*

Department of Applied Mathematics, University of Leeds, Leeds, LS2 9JT, United Kingdom

Abstract

We consider the inverse bio-heat transfer problem to determine the space- and time-dependent perfusion coefficient from temperature measurements. In this formulation, the problem is fully determined and the coefficient is identifiable if and only if the temperature has dense support. However, the problem is still ill-posed since small errors in the measured temperature cause large errors in the output perfusion coefficient due to the numerical differentiation of noisy data involved which represents an unstable procedure. In order to overcome this difficulty and restore stability, we employ for the first time the conjugate gradient method (CGM) for solving the inverse problem under investigation. Regularization is achieved by stopping the iteration process at an appropriate threshold dictated by the discrepancy principle. Numerical results show that the CGM is accurate and reasonably stable in retrieving the perfusion coefficient. Moreover, comparison with other methods shows improved efficiency and stability in inverting noisy data.

Keywords: inverse problem, bio-heat equation, ill-posed problem, conjugate gradient method, perfusion coefficient

2010 MSC: 65M32, 35K05

1. Introduction

Despite much work carried out to understand interactions that occur in perfused tissues during thermal treatments, [1, 2, 3, 4], there is still of great importance to identify how the convective heat transport is modelled by blood perfusion, [5]. Therefore, in this paper, we consider a one-dimensional inverse bio-heat conduction problem to determine the space- and time-dependent blood perfusion coefficient from temperature measurements which would be of very much interest to bio-medical engineering applications such as, e.g. hyperthermia cancer therapy. In the direct problem, the cause (perfusion coefficient) is given and the effect (temperature field) is determined. However, the inverse problem involves the estimation of the cause from the knowledge of the effect.

Difficulties encountered in the solution of the inverse heat transfer problems should be recognized, since, in general, they are ill-posed, see [6, 7]. The solution of a well-posed problem needs

*Corresponding author

Email addresses: mmkc@leeds.ac.uk (K. Cao), amt51d@maths.leeds.ac.uk (D. Lesnic)

to satisfy the requirements of existence, uniqueness and stability with respect to the input data. The existence of a solution for an inverse problem may be assured according to physical reasoning. However, the uniqueness of the solution can be mathematically proved only under further restrictions or assumptions. Further, the solutions may become unstable, as a result of the errors which are inherently present in the practical measurements.

The mathematical formulation of the coefficient identification problem under investigation is presented in Section 2. The numerical conjugate gradient method (CGM) for solving it is presented in Section 3. Numerical results are presented and discussed in Section 4 and finally, Section 5 highlights the conclusions of the work.

2. The mathematical formulation

Understanding the thermal life behaviour and temperature distribution in living tissues are key tasks in modern clinical treatments of cancer hyperthermia or skin burn injuries using thermotherapy, [8, 9]. The blood flow exchanged through tissue plays an important role in the temperature regulatory system of the human body, [1]. The governing equation describing the relation between the tissue temperature and the arterial blood perfusion is given by the transient bio-heat equation, [2]. We solve this equation in a finite slab $\Omega = (0, 1)$, over the time interval from the initial time $t = 0$ to the final time $t = t_f$,

$$\frac{\partial T}{\partial t}(x, t) = \frac{\partial}{\partial x} \left(k(x, t) \frac{\partial T}{\partial x}(x, t) \right) - q(x, t)T(x, t) + S(x, t), \quad (x, t) \in (0, 1) \times (0, t_f), \quad (1)$$

subject to the Neumann boundary conditions

$$-k(0, t) \frac{\partial T}{\partial x}(0, t) = q_1(t), \quad k(1, t) \frac{\partial T}{\partial x}(1, t) = q_2(t), \quad t \in (0, t_f), \quad (2)$$

and the initial condition

$$T(x, 0) = T_0(x), \quad x \in [0, 1], \quad (3)$$

where $k(x, t) > 0$ is the thermal conductivity, $q(x, t) \geq 0$ is the perfusion coefficient, $T(x, t)$ represents the temperature, $S(x, t)$ is the source term, $q_1(t)$ and $q_2(t)$ are heat fluxes and $T_0(x)$ is the initial temperature. For simplicity, the heat capacity has been assumed constant and taken to be equal to unity. Dirichlet, mixed or Robin boundary conditions can be prescribed instead of the Neumann heat flux boundary conditions (2).

The perfusion coefficient q incorporates information about the blood perfusion rate and plays an important role in the temperature regulatory system of the human body, [1, 10]. Note also that equation (1) occurs in other applications such as those related to diffusion optical tomography, [11].

The direct problem is concerned with the determination of the temperature field $T(x, t)$ in the region $[0, 1] \times [0, t_f]$ by solving (1)–(3) when the coefficients $k(x, t)$ and $q(x, t)$ are known. The inverse problem, on the other hand, is concerned with the determination of the unknown perfusion coefficient $q(x, t) \geq 0$ from the knowledge of the temperature $T(x, t)$.

The identification of the perfusion coefficient, being constant or dependent on time or space only, from limited measurements of the temperature, heat flux or energy has been investigated in, e.g. [12, 13, 14], but in this study we investigate the more general case concerned with the inversion of the mapping $q(x, t) \mapsto T(x, t)$. This inverse problem has previously been investigated in [10] using stabilisations of the partial derivatives present in the explicit formula, see (1),

$$q(x, t) = \frac{\frac{\partial k}{\partial x}(x, t) \frac{\partial T}{\partial x}(x, t) + k(x, t) \frac{\partial^2 T}{\partial x^2}(x, t) - \frac{\partial T}{\partial t}(x, t) + S(x, t)}{T(x, t)}, \quad (x, t) \in (0, 1) \times (0, t_f). \quad (4)$$

One can also mention the time semi-discrete scheme of [15], through which the problem is transformed into a sequence of inverse problems with solely space-dependent unknown coefficients, and the first-order Tikhonov regularization method of [16]. We mention that no numerical tests have been attempted in these works, [15, 16].

From (4), one can observe that $q(x, t)$ is identifiable if and only if the set $\{(x, t) \in (0, 1) \times (0, t_f); T(x, t) = 0\}$ has zero measure. In this study, we avoid the use of the unstable formula (4) by reformulating the inverse problem as a least-squares minimization which is then solved numerically using the regularizing CGM, where the stabilisation is achieved by stopping the iterations according to the discrepancy principle. This is the main novelty and contribution of our paper.

Let $T(x, t; q)$ denote the solution of the direct problem, that is, the temperature corresponding to a particular perfusion coefficient $q(x, t)$. Let the temperature readings at the uniform space locations $x_i = \frac{i-1}{I-1}$ be denoted by $Y(x_i, t; q) \equiv Y_i(t)$ for $i = \overline{1, I}$. We note that the measured data may contain noisy errors. The solution of the inverse problem is to be obtained in such a way that the following least-squares functional is minimized:

$$J[q] = \frac{1}{2} \sum_{i=1}^I \|T(x_i, t; q) - Y_i(t)\|_{L^2[0, t_f]}^2 = \frac{1}{2} \int_0^{t_f} \sum_{i=1}^I [T(x_i, t; q) - Y_i(t)]^2 dt. \quad (5)$$

The minimization of (5) is performed using the CGM, as described in the next section.

3. The conjugate gradient method (CGM)

The CGM is an iterative method formed of three problems, [17], namely: the direct problem, the sensitivity problem which will be described in Subsection 3.1 and the adjoint problem which will be described in Subsection 3.2.

3.1. The sensitivity problem

The sensitivity problem is obtained from the direct problem using the following approach. Let us suppose that the temperature distribution $T(x, t)$ is perturbed by $\varepsilon \Delta T(x, t)$ when the perfusion coefficient $q(x, t)$ is perturbed by $\varepsilon \Delta q(x, t)$, where $\varepsilon > 0$ is a small number. Subtracting the two corresponding direct problems, dividing with ε , and letting $\varepsilon \searrow 0$, we obtain the sensitivity problem given by

$$\frac{\partial(\Delta T)}{\partial t}(x, t) = \frac{\partial}{\partial x} \left(k(x, t) \frac{\partial(\Delta T)}{\partial x}(x, t) \right) - q(x, t) \Delta T(x, t) - T(x, t) \Delta q(x, t), \quad (x, t) \in (0, 1) \times (0, t_f), \quad (6)$$

$$-k(0, t) \frac{\partial(\Delta T)}{\partial x}(0, t) = 0, \quad k(1, t) \frac{\partial(\Delta T)}{\partial x}(1, t) = 0, \quad t \in (0, t_f), \quad (7)$$

$$\Delta T(x, 0) = 0, \quad x \in [0, 1]. \quad (8)$$

3.2. The adjoint problem

We can write the minimization of the functional $J[q]$ as a constrained optimization problem, since the estimated temperature $T(x, t; q(x, t))$ must satisfy the direct problem. In order to solve this constrained optimization problem, we use the Lagrange multiplier method. This yields the following extended objective functional:

$$J[q] = \frac{1}{2} \int_0^{t_f} \sum_{i=1}^I [T(x_i, t; q) - Y_i(t)]^2 dt + \int_0^{t_f} \int_0^1 \lambda(x, t) \left\{ \frac{\partial}{\partial x} \left[k(x, t) \frac{\partial T}{\partial x}(x, t) \right] - q(x, t) T(x, t) + S(x, t) - \frac{\partial T}{\partial t}(x, t) \right\} dx dt, \quad (9)$$

where $\lambda(x, t)$ is a Lagrange multiplier. Note that we can use the Dirac delta function δ to rewrite (9) as

$$J[q] = \frac{1}{2} \int_0^{t_f} \left([T(x_1, t; q) - Y_1(t)]^2 + [T(x_I, t; q) - Y_I(t)]^2 \right) dt + \frac{1}{2} \int_0^{t_f} \int_0^1 \sum_{i=2}^{I-1} [T(x_i, t; q) - Y_i(t)]^2 \delta(x - x_i) dx dt + \int_0^{t_f} \int_0^1 \lambda(x, t) \left\{ \frac{\partial}{\partial x} \left[k(x, t) \frac{\partial T}{\partial x}(x, t) \right] - q(x, t) T(x, t) + S(x, t) - \frac{\partial T}{\partial t}(x, t) \right\} dx dt. \quad (10)$$

Then, we can define the directional derivative of $J[q]$ in the direction of the perturbation in q as

$$\Delta J[q] = \lim_{\varepsilon \searrow 0} \frac{J[q_\varepsilon] - J[q]}{\varepsilon}, \quad (11)$$

where

$$J[q_\varepsilon] = \frac{1}{2} \int_0^{t_f} \left([T + \varepsilon \Delta T - Y_1]^2 + [T + \varepsilon \Delta T - Y_I]^2 \right) dt + \frac{1}{2} \int_0^{t_f} \int_0^1 \sum_{i=2}^{I-1} [T + \varepsilon \Delta T - Y_i]^2 \delta(x - x_i) dx dt + \int_0^{t_f} \int_0^1 \lambda(x, t) \left\{ \frac{\partial}{\partial x} \left[k \frac{\partial(T + \varepsilon \Delta T)}{\partial x} \right] - (q + \varepsilon \Delta q)(T + \varepsilon \Delta T) + S - \frac{\partial(T + \varepsilon \Delta T)}{\partial t} \right\} dx dt.$$

Now expanding the term $[T + \varepsilon \Delta T - Y_i]^2$ and neglecting the second-order terms of order ε^2 in the expression, we obtain

$$[T + \varepsilon \Delta T - Y_i]^2 \approx T^2 + Y_i^2 - 2Y_i T + 2\varepsilon T \Delta T - 2\varepsilon Y_i \Delta T = (T - Y_i)^2 + 2\varepsilon \Delta T (T - Y_i)$$

and then

$$J[q_\varepsilon] = \frac{1}{2} \int_0^{t_f} \left([(T - Y_1)^2 + 2\varepsilon \Delta T (T - Y_1)] + [(T - Y_I)^2 + 2\varepsilon \Delta T (T - Y_I)] \right) dt + \frac{1}{2} \int_0^{t_f} \int_0^1 \sum_{i=2}^{I-1} [(T - Y_i)^2 + 2\varepsilon \Delta T (T - Y_i)] \delta(x - x_i) dx dt + \int_0^{t_f} \int_0^1 \lambda(x, t) \left\{ \frac{\partial}{\partial x} \left[k \frac{\partial(T + \varepsilon \Delta T)}{\partial x} \right] - (q + \varepsilon \Delta q)(T + \varepsilon \Delta T) + S - \frac{\partial(T + \varepsilon \Delta T)}{\partial t} \right\} dx dt.$$

Now subtracting $J[q]$ from $J[q_\varepsilon]$, and neglecting the second-order terms of order ε^2 , we have

$$\begin{aligned} J[q_\varepsilon] - J[q] &= \int_0^{t_f} \varepsilon \Delta T [(T - Y_1) + (T - Y_I)] dt + \int_0^{t_f} \int_0^1 \sum_{i=2}^{I-1} \varepsilon \Delta T (T - Y_i) \delta(x - x_i) dx dt \\ &\quad + \int_0^{t_f} \int_0^1 \lambda(x, t) \left\{ \frac{\partial}{\partial x} \left[k \frac{\partial(\varepsilon \Delta T)}{\partial x} \right] - \varepsilon q \Delta T - \varepsilon T \Delta q - \frac{\partial(\varepsilon \Delta T)}{\partial t} \right\} dx dt. \end{aligned}$$

Using (11), we obtain

$$\begin{aligned} \Delta J[q] &= \int_0^{t_f} \Delta T [(T - Y_1) + (T - Y_I)] dt + \int_0^{t_f} \int_0^1 \sum_{i=2}^{I-1} \Delta T (T - Y_i) \delta(x - x_i) dx dt \\ &\quad + \int_0^{t_f} \int_0^1 \lambda(x, t) \left\{ \frac{\partial}{\partial x} \left[k \frac{\partial(\Delta T)}{\partial x} \right] - q \Delta T - T \Delta q - \frac{\partial(\Delta T)}{\partial t} \right\} dx dt. \end{aligned} \quad (12)$$

Let us analyse each one of the integrals in (12). We have

$$\begin{aligned} I_1 &= \int_0^{t_f} \int_0^1 \lambda \frac{\partial}{\partial x} \left[k \frac{\partial(\Delta T)}{\partial x} \right] dx dt = \int_0^{t_f} \left[\lambda k \frac{\partial(\Delta T)}{\partial x} \Big|_0^1 - \int_0^1 k \frac{\partial(\Delta T)}{\partial x} \frac{\partial \lambda}{\partial x} dx \right] dt \\ &= \int_0^{t_f} \left[\lambda k \frac{\partial(\Delta T)}{\partial x} \Big|_0^1 - k \Delta T \frac{\partial \lambda}{\partial x} \Big|_0^1 + \int_0^1 \Delta T \frac{\partial}{\partial x} \left[k \frac{\partial \lambda}{\partial x} \right] dx \right] dt \end{aligned}$$

and

$$I_2 = \int_0^{t_f} \int_0^1 \lambda \frac{\partial(\Delta T)}{\partial t} dx dt = \int_0^1 \left[\lambda \Delta T \Big|_0^{t_f} - \int_0^{t_f} \Delta T \frac{\partial \lambda}{\partial t} dt \right] dx.$$

Substituting the integrals from I_1 and I_2 into (12), we obtain

$$\begin{aligned} \Delta J[q] &= \int_0^{t_f} \int_0^1 \Delta T \left\{ \sum_{i=2}^{I-1} (T - Y_i) \delta(x - x_i) + \frac{\partial}{\partial x} \left[k \frac{\partial \lambda}{\partial x} \right] - q \lambda + \frac{\partial \lambda}{\partial t} \right\} dx dt \\ &\quad + \int_0^{t_f} \Delta T [(T - Y_1) + (T - Y_I)] dt + \int_0^{t_f} \left[\lambda k \frac{\partial(\Delta T)}{\partial x} \Big|_0^1 - k \Delta T \frac{\partial \lambda}{\partial x} \Big|_0^1 \right] dt \\ &\quad - \int_0^{t_f} \int_0^1 \lambda T \Delta q dx dt - \int_0^1 \lambda \Delta T \Big|_0^{t_f} dx. \end{aligned} \quad (13)$$

Using (7) and (8), the vanishing of the integrands containing ΔT in (13) leads to the following adjoint problem for the determination of the Lagrange multiplier $\lambda(x, t)$:

$$\begin{aligned} \frac{\partial \lambda}{\partial t}(x, t) &= -\frac{\partial}{\partial x} \left[k(x, t) \frac{\partial \lambda}{\partial x}(x, t) \right] + q(x, t) \lambda(x, t) - \sum_{i=2}^{I-1} (T(x_i, t; q) - Y_i(t)) \delta(x - x_i), \\ &\quad (x, t) \in (0, 1) \times (0, t_f), \end{aligned} \quad (14)$$

$$-k(0, t) \frac{\partial \lambda}{\partial x}(0, t) = T(0, t; q) - Y_1(t), \quad k(1, t) \frac{\partial \lambda}{\partial x}(1, t) = T(1, t; q) - Y_I(t), \quad t \in (0, t_f), \quad (15)$$

$$\lambda(x, t_f) = 0, \quad x \in [0, 1]. \quad (16)$$

The following term remains in (13)

$$\Delta J[q] = - \int_0^{t_f} \int_0^1 \lambda(x, t) T(x, t) \Delta q(x, t) dx dt, \quad (17)$$

and we know that

$$\Delta J[q] = \int_0^{t_f} \int_0^1 J'[q] \Delta q(x, t) dx dt. \quad (18)$$

Thus, by (17) and (18) we find that the gradient of the functional $J[q]$ is

$$J'[q] = -\lambda(x, t)T(x, t). \quad (19)$$

3.3. Iteration procedure

The following iterative process based on the CGM is now used for the estimation of $q(x, t)$ by minimizing the objective functional $J[q]$:

$$q^{n+1}(x, t) = q^n(x, t) - \beta^n P^n(x, t), \quad n = 0, 1, 2, \dots, \quad (20)$$

where the superscript n denotes the iteration number, q^0 is an initial guess, β^n is the step search size and P^n is the direction of descent given by

$$P^0(x, t) = J'[q^0(x, t)], \quad P^n(x, t) = J'[q^n(x, t)] + \gamma^n P^{n-1}(x, t), \quad n = 1, 2, \dots. \quad (21)$$

Different expressions are available for the conjugate coefficient γ^n . The Polak–Ribiere expression [6, 18] is given by

$$\gamma^0 = 0, \quad \gamma^n = \frac{\int_0^{t_f} \int_0^1 J'[q^n(x, t)] \{J'[q^n(x, t)] - J'[q^{n-1}(x, t)]\} dx dt}{\int_0^{t_f} \int_0^1 \{J'[q^{n-1}(x, t)]\}^2 dx dt}, \quad n = 1, 2, \dots, \quad (22)$$

while the Fletcher–Reeves [6, 18, 19] expression is given by

$$\gamma^0 = 0, \quad \gamma^n = \frac{\int_0^{t_f} \int_0^1 \{J'[q^n(x, t)]\}^2 dx dt}{\int_0^{t_f} \int_0^1 \{J'[q^{n-1}(x, t)]\}^2 dx dt}, \quad n = 1, 2, \dots. \quad (23)$$

The search step size β^n is found from the condition

$$\beta^n = \min_{\beta} J(q^n - \beta P^n). \quad (24)$$

Let us set $\Delta q^n = P^n$, and by using the definition of the functional $J[q]$ in (5) and linearising $T(x_i, t; q^n - \beta P^n) \approx T(x_i, t; q^n) - \beta \Delta T_i^n$, where the sensitivity function $\Delta T_i^n(t) = \Delta T(x_i, t; P^n)$ is obtained by solving the sensitivity problem (6)–(8) with $\Delta q^n = P^n$, see [20], we have

$$\begin{aligned} J(q^n - \beta P^n) &= \frac{1}{2} \int_0^{t_f} \sum_{i=1}^I [T(x_i, t; q^n - \beta P^n) - Y_i(t)]^2 dt \\ &= \frac{1}{2} \int_0^{t_f} \sum_{i=1}^I [T(x_i, t; q^n) - \beta \Delta T_i^n - Y_i(t)]^2 dt. \end{aligned}$$

Then, we calculate the derivative of $J(q^n - \beta P^n)$ with respect to β and obtain

$$\frac{\partial J}{\partial \beta} = - \int_0^{t_f} \sum_{i=1}^I [T(x_i, t; q^n) - \beta \Delta T_i^n - Y_i(t)] \Delta T_i^n dt.$$

Next, we set $\frac{\partial J}{\partial \beta} = 0$ and obtain the search step size β^n as follows:

$$\beta^n = \frac{\int_0^{t_f} \sum_{i=1}^I [T(x_i, t; q^n) - Y_i(t)] \Delta T_i^n dt}{\int_0^{t_f} \sum_{i=1}^I (\Delta T_i^n)^2 dt}. \quad (25)$$

3.4. The stopping criterion

The iterative procedure given by equation (20) does not provide the CGM with the stabilization necessary for the minimization of the objective functional (5) to be classified as well-posed because of the errors in the measured temperature. However, the CGM may become well-posed if the discrepancy principle is used to stop the iterative procedure. In this criterion, the iterative procedure is stopped when

$$J[q^n] \approx \frac{1}{2}\mu^2, \quad (26)$$

where

$$\mu = \sqrt{\int_0^{t_f} \sum_{i=1}^I [Y_i(t) - Y_i^{exact}(t)]^2 dt}, \quad (27)$$

represents the amount of noise in the measured temperature.

3.5. Algorithm

The steps of the CGM algorithm are as follows:

- 1 Choose an initial guess $q^0(x, t)$ and set $n = 0$.
- 2 Solve the direct problem to obtain $T(x_i, t; q^n)$, and compute $J[q^n]$ by equation (5).
- 3 Solve the adjoint problem (14)–(16) to compute the Lagrange multiplier $\lambda(x, t; q^n)$, and the gradient $J'[q^n]$ from the equation (19). Compute the conjugate coefficient γ^n from (23), and the direction of descent P^n from (21).
- 4 Solve the sensitivity problem (6)–(8) to obtain the sensitivity function $\Delta T(x_i, t; q^n)$ by taking $\Delta q^n = P^n$, and compute the search step size β^n from (25).
- 5 Compute $q^{n+1}(x, t)$ from (20).
- 6 The stopping condition (26) is:
 If $J[q^n] \approx \frac{1}{2}\mu^2$ go to step 7.
 Else set $n = n + 1$ and go to step 2.
- 7 End.

4. Numerical results and discussion

In this section we perform numerical experiments based on the CGM described in the previous section. First, we set $n = 0$ and choose an arbitrary initial guess $q^0(x, t)$.

For numerical discretisation, we construct a rectangular network of mesh size Δx over the region and consider the time step of size Δt ,

$$x_i = (i - 1)\Delta x, \quad i = \overline{1, I}, \quad \Delta x = \frac{1}{I - 1}, \quad (28)$$

$$t_l = (l - 1)\Delta t, \quad l = \overline{1, L}, \quad \Delta t = \frac{t_f}{L - 1}. \quad (29)$$

We approximate

$$\begin{aligned} \left. \frac{\partial}{\partial x} \left(k \frac{\partial T}{\partial x} \right) \right|_{i,l} &\simeq \frac{k_{i+1/2}^l \left(\frac{T_{i+1}^l - T_i^l}{\Delta x} \right) - k_{i-1/2}^l \left(\frac{T_i^l - T_{i-1}^l}{\Delta x} \right)}{\Delta x} \\ &= \frac{k_{i+1/2}^l}{(\Delta x)^2} T_{i+1}^l - \frac{k_{i+1/2}^l + k_{i-1/2}^l}{(\Delta x)^2} T_i^l + \frac{k_{i-1/2}^l}{(\Delta x)^2} T_{i-1}^l, \end{aligned} \quad (30)$$

and employ the Crank-Nicolson finite-difference method (FDM), [21], to discretise the partial differential bio-heat equation (1) as

$$\begin{aligned} \frac{T_i^{l+1} - T_i^l}{\Delta t} &= \frac{1}{2} \left\{ \frac{k_{i+1/2}^{l+1}}{(\Delta x)^2} T_{i+1}^{l+1} - \frac{k_{i+1/2}^{l+1} + k_{i-1/2}^{l+1}}{(\Delta x)^2} T_i^{l+1} + \frac{k_{i-1/2}^{l+1}}{(\Delta x)^2} T_{i-1}^{l+1} - q_i^{l+1} T_i^{l+1} + S_i^{l+1} \right. \\ &\quad \left. + \frac{k_{i+1/2}^l}{(\Delta x)^2} T_{i+1}^l - \frac{k_{i+1/2}^l + k_{i-1/2}^l}{(\Delta x)^2} T_i^l + \frac{k_{i-1/2}^l}{(\Delta x)^2} T_{i-1}^l - q_i^l T_i^l + S_i^l \right\}. \end{aligned} \quad (31)$$

This leads to

$$\begin{aligned} &-\alpha_{i-1/2}^{l+1} T_{i-1}^{l+1} + (2 + \alpha_{i-1/2}^{l+1} + \alpha_{i+1/2}^{l+1} + q_i^{l+1} \Delta t) T_i^{l+1} - \alpha_{i+1/2}^{l+1} T_{i+1}^{l+1} \\ &= \alpha_{i-1/2}^l T_{i-1}^l + (2 - \alpha_{i-1/2}^l - \alpha_{i+1/2}^l - q_i^l \Delta t) T_i^l + \alpha_{i+1/2}^l T_{i+1}^l + \Delta t (S_i^l + S_i^{l+1}), \end{aligned} \quad (32)$$

where $\alpha(x, t) = k(x, t) \Delta t / (\Delta x)^2$ and $\alpha_{i\pm 1/2}^l = (\alpha_i^l + \alpha_{i\pm 1}^l) / 2$.

Thus, the above formulation can be written as:

$$A \mathbf{T}^{l+1} = \mathbf{f}^l, \quad l = \overline{1, L-1}, \quad (33)$$

where $A = (a_{ij})_{I \times I}$ is a tridiagonal matrix,

$$\begin{aligned} a_{i,i} &= 2 + \alpha_{i-\frac{1}{2}}^{l+1} + \alpha_{i+\frac{1}{2}}^{l+1} + q_i^{l+1} \Delta t, \quad i = \overline{1, I}, \\ a_{i,i-1} &= -\alpha_{i-\frac{1}{2}}^{l+1}, \quad a_{i,i+1} = -\alpha_{i+\frac{1}{2}}^{l+1}, \quad i = \overline{2, I-1}, \\ a_{1,2} &= -(\alpha_{\frac{1}{2}}^{l+1} + \alpha_{\frac{3}{2}}^{l+1}), \quad a_{I,I-1} = -(\alpha_{I-\frac{1}{2}}^{l+1} + \alpha_{I+\frac{1}{2}}^{l+1}), \end{aligned}$$

$\mathbf{T}^{l+1} = [T_1^{l+1}, T_2^{l+1}, \dots, T_I^{l+1}]^T$, \mathbf{T}^1 is determined by $T_0(x)$, $\mathbf{f}^l = [f_1^l, f_2^l, \dots, f_I^l]^T$, and

$$\begin{aligned} f_1^l &= 2\alpha_{1/2}^{l+1} (q_1^{l+1} / k_1^{l+1}) \Delta x + \alpha_{1/2}^l T_0^l + (2 - \alpha_{1/2}^l - \alpha_{3/2}^l - q_1^l \Delta t) T_1^l + \alpha_{3/2}^l T_2^l + \Delta t (S_1^l + S_1^{l+1}), \\ f_i^l &= \alpha_{i-1/2}^l T_{i-1}^l + (2 - \alpha_{i-1/2}^l - \alpha_{i+1/2}^l - q_i^l \Delta t) T_i^l + \alpha_{i+1/2}^l T_{i+1}^l + \Delta t (S_i^l + S_i^{l+1}), \\ &\quad i = \overline{2, I-1}, \\ f_I^l &= \alpha_{I-1/2}^l T_{I-1}^l + (2 - \alpha_{I-1/2}^l - \alpha_{I+1/2}^l - q_I^l \Delta t) T_I^l + \alpha_{I+1/2}^l T_{I+1}^l + 2\alpha_{I+1/2}^{l+1} (q_2^{l+1} / k_I^{l+1}) \Delta x \\ &\quad + \Delta t (S_I^l + S_I^{l+1}), \end{aligned}$$

where $T_0^l = T_2^l + 2(q_1^l / k_1^l) \Delta x$ and $T_{I+1}^l = T_{I-1}^l + 2(q_2^l / k_I^l) \Delta x$ by using the Neumann boundary conditions (2).

We can use the above FDM to solve the direct, sensitivity and adjoint problems. Note that in the adjoint problem, the equation (14) contains the Dirac delta function which can be approximated by

$$\delta(x - x_i) \approx \frac{1}{a\sqrt{\pi}} e^{-(x-x_i)^2/a^2}, \quad i = \overline{1, I}, \quad (34)$$

where a is a small positive constant. The trapezoidal rule is used to approximate all the integrations involved, e.g. for the objective functional (5), we have

$$\begin{aligned} J[q] &= \frac{1}{2} \sum_{i=1}^I \|T(x_i, t; q) - Y_i(t)\|_{L^2[0, t_f]}^2 \\ &\approx \frac{\Delta t}{4} \sum_{i=1}^I \left\{ (T(x_i, t_1; q) - Y_{i,1})^2 + 2 \sum_{l=2}^{L-1} (T(x_i, t_l; q) - Y_{i,l})^2 + (T(x_i, t_L; q) - Y_{i,L})^2 \right\}, \end{aligned} \quad (35)$$

where $Y_{i,l} = Y_i(t_l)$. Note also that $T(x_i, t_1; q) = Y_{i,1} = T_0(x_i)$ for $i = \overline{1, I}$, is given from (3).

We define the error functional at the iteration number n for the perfusion coefficient $q(x, t)$ as

$$E(q^n) = \sqrt{\frac{1}{IL} \sum_{i=1}^L \sum_{l=1}^I (q_{i,l}^n - q_{i,l}^{exact})^2}. \quad (36)$$

The measurements Y containing random errors are simulated by adding to Y^{exact} an error term generated from a normal distribution by MATLAB in the form:

$$Y = Y^{exact} + \text{random}('Normal', 0, \sigma, I, L), \quad (37)$$

where $\sigma = \frac{p}{100} \max_{0 \leq x \leq 1, 0 \leq t \leq t_f} |T(x, t)|$ is the standard deviation and $p\%$ is the percentage of noise.

Note that from (16) and (19), $J'(x, t_f)$ always equals zero. Therefore, if the final time values of $q(x, t_f)$ cannot be predicted before the inverse calculation, the estimated values of $q(x, t)$ will deviate from the exact values near the final time, [20]. Generally speaking, there are two methods to avoid it, one is to use the modified CGM, [22], and the other one is to record data a little longer than the actual period of interest. In this paper, we use the second method and take $t'_f = 1.2$ as the longer time than the actual final time $t_f = 1$.

In the following, we present the numerical results obtained with a FDM mesh size of $\Delta x = \Delta t = 0.01$.

4.1. Example 1

We take the input data as

$$q_1(t) = e^{-t}(2t + 4), \quad q_2(t) = -e^{-(t+1)}(2t + 3), \quad (38)$$

$$k(x, t) = 1, \quad T_0(x) = e^{-x}(x^2 + 4), \quad S(x, t) = 0, \quad (39)$$

$$T(x, t) = Y^{exact}(x, t) = e^{-(x+t)}(2t + x^2 + 4). \quad (40)$$

The analytical solution of the inverse problem is given by

$$q(x, t) = 2 - \frac{4x}{2t + x^2 + 4}. \quad (41)$$

We take the initial guess $q^0(x, t) = 1$.

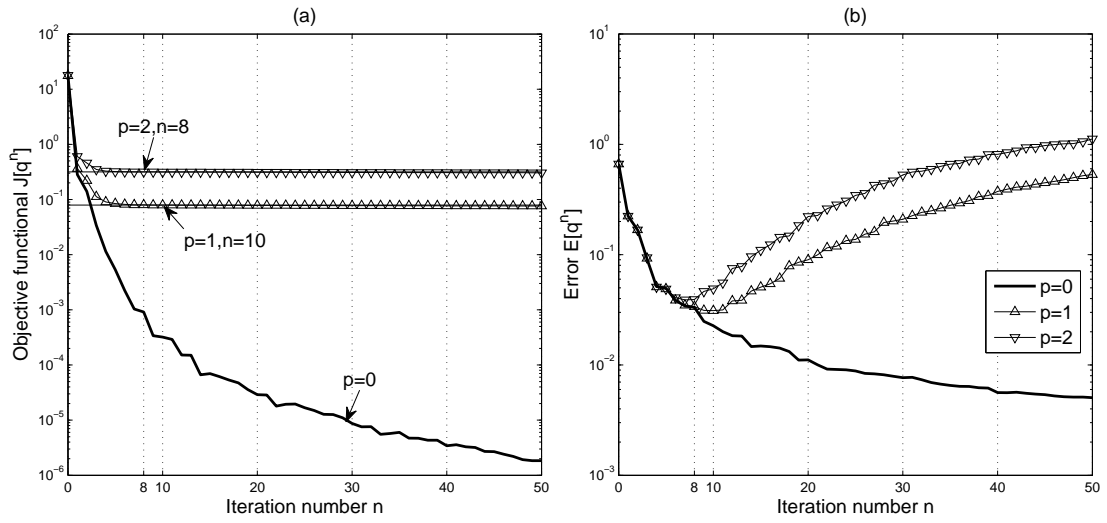


Figure 1: (a) The objective functional $J(q^n)$ and (b) the error $E(q^n)$ for $p \in \{0, 1, 2\}$, for *Example 1*.

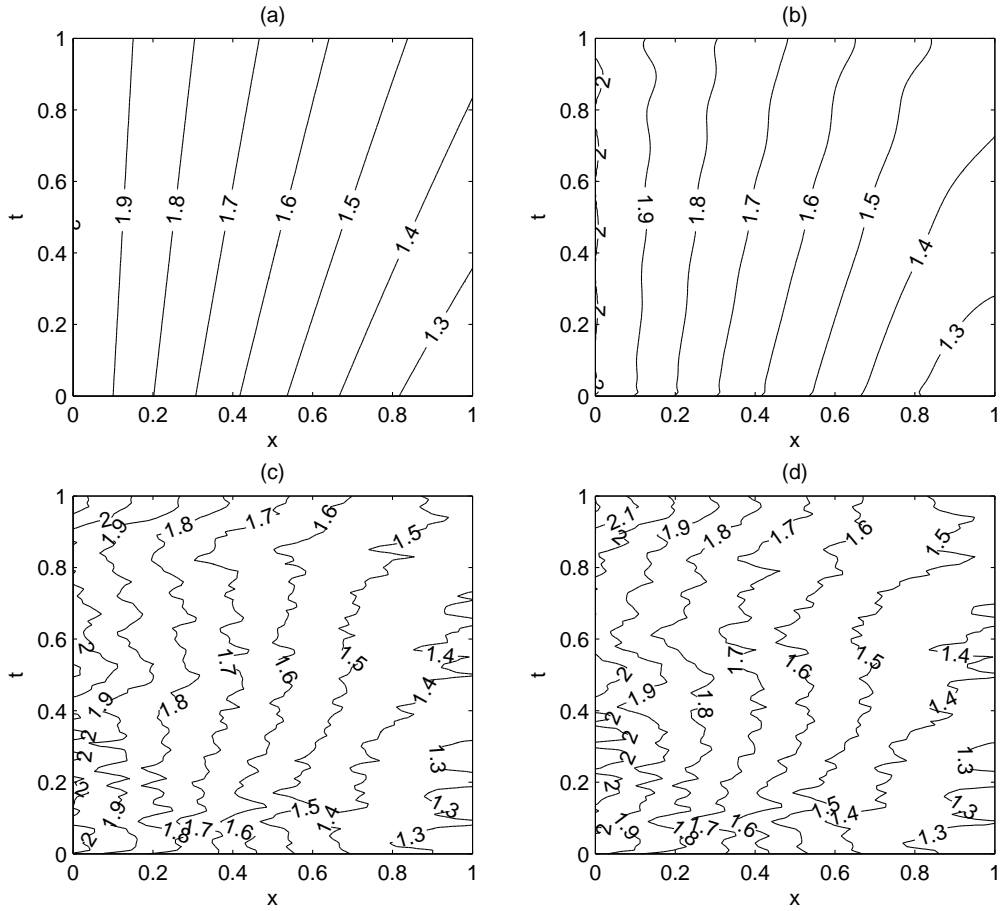


Figure 2: (a) The exact and estimated perfusion coefficient $q(x, t)$ for (b) $p = 0$, (c) $p = 1$, and (d) $p = 2$, for *Example 1*.

Figure 1(a) shows the monotonic decreasing convergence of the objective functional (5) that is minimized, as a function of the number of iterations n , for various amounts of noise $p = 0$

(no noise) and $p\% \in \{1, 2\}\%$ noisy data (37). For noisy data, the intersection of horizontal lines $y = \frac{1}{2}\mu^2(p)$, where $\mu(p)$ is given by (27), with the graphs of $J[q^n]$ yields the stopping iteration numbers $n_d(p) \in \{10, 8\}$ for $p \in \{1, 2\}$, respectively, according to the discrepancy principle (26). These values can then be compared with the optimal ones of $n_{opt}(p) \in \{10, 7\}$ for $p \in \{1, 2\}$, respectively, obtained by plotting the error curves $E(q^n) = \|q^n - q\|_{L^2(0,1)}$, as functions of the number of iterations n , in Figure 1(b). The comparison shows that n_d and n_{opt} are close to each other. Of course, in practice only the values of n_d can be calculated according to the discrepancy principle (26).

The numerical results are illustrated in Figure 2. In the case of no noise in Figure 2(b), the results are plotted after 50 iterations, whilst for noisy data the results are plotted after $n_d(p)$ iterations. First, from Figure 2(b) it can be seen that in the case of no noise, the retrieved solution is in very good agreement with the exact solution in Figure 2(a). Second, from Figures 2(c) and 2(d) it can be seen that in the case of noisy data, the retrieved solution is reasonably stable and it becomes more accurate as the amount of noise p decreases.

We finally note that *Example 1* has also been considered in [10] using the nonlinear Tikhonov regularization, as well as a local approach based on regularizing the numerical differentiation (once in time and twice in space) of the noisy measured temperature (37). On comparing the results of [10] with the CGM results in Figure 2 it is reported that both methods yield accurate results for exact data, i.e. $p = 0$, but the latter one is more stable when inverting noisy data.

4.2. Example 2

We take the input data as

$$q_1(t) = -\frac{2\pi+1}{12}e^{-t}(1+t), \quad q_2(t) = \frac{2+t}{12}e^{-t}, \quad (42)$$

$$k(x, t) = \frac{1+x+t}{12}, \quad T_0(x) = \sin(\pi x) + (\pi+1)x + 1, \quad (43)$$

$$S(x, t) = -e^{-t}(\sin(\pi x) + (\pi+1)x + 1) - \frac{e^{-t}}{12}(\pi \cos(\pi x) + \pi + 1) \\ + \frac{\pi^2}{12}(1+x+t)e^{-t}\sin(\pi x) + (1+x+t)e^{-t}(\sin(\pi x) + (\pi+1)x + 1). \quad (44)$$

$$T(x, t) = Y^{exact}(x, t) = e^{-t}(\sin(\pi x) + (\pi+1)x + 1). \quad (45)$$

In contrast to the previous example corresponding to a homogeneous tissue with constant thermal conductivity, this example characterises a heterogeneous tissue with the thermal conductivity $k(x, t) = (1+x+t)/12$ depending on both space and time.

The analytical solution of the inverse problem is given by

$$q(x, t) = 1 + x + t. \quad (46)$$

We take the initial guess $q^0(x, t) = 1$.

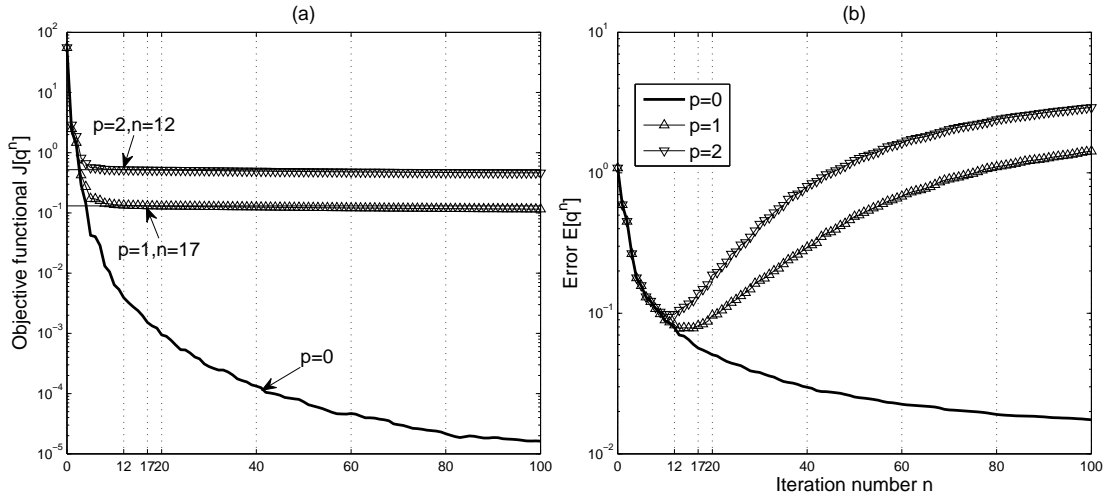


Figure 3: (a) The objective functional $J(q^n)$ and (b) the error $E(q^n)$ for $p \in \{0, 1, 2\}$, for *Example 2*.

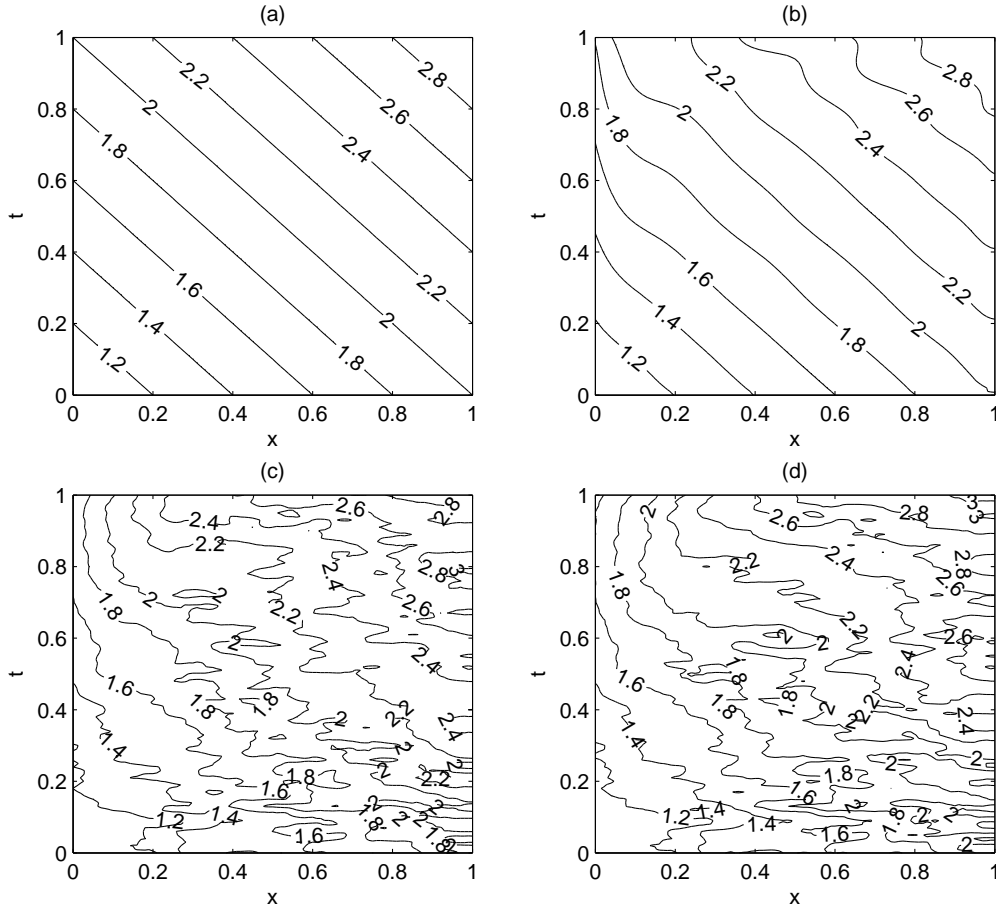


Figure 4: (a) The exact and estimated perfusion coefficient $q(x, t)$ with (b) $p = 0$, (c) $p = 1$, and (d) $p = 2$, for *Example 2*.

Figure 3(a) shows the monotonic decreasing convergence of the objective functional (5), as a function of the number of iterations n , for various amounts of noise $p = 0$ (no noise) and $p\% \in \{1, 2\}\%$ noisy data (37). For noisy data, the intersection of horizontal lines $y = \frac{1}{2}\mu^2(p)$,

with the graphs of $J[q^n]$ yields the stopping iteration numbers $n_d(p) \in \{17, 12\}$ for $p \in \{1, 2\}$, respectively, according to the discrepancy principle (26). These values can then be compared with the optimal ones of $n_{opt}(p) \in \{13, 11\}$ for $p \in \{1, 2\}$, respectively, obtained by plotting the error curves $E(q^n) = \|q^n - q\|_{L^2(0,1)}$, as functions of the number of iterations n , in Figure 3(b). Although for $p > 0$, n_d and n_{opt} are not as close to each other as in *Example 1*, Figure 3(b) illustrates that the valley of minima of the error $E(q^n)$ is rather flat over some range of iterations before it diverges.

The numerical results for the perfusion coefficient are illustrated in Figure 4. In the case of no noise in Figure 4(b), the results are plotted after 100 iterations, whilst for noisy data the results are plotted after $n_d(p)$ iterations. First, from Figure 4(b) it can be seen that in the case of no noise, the retrieved solution is in very good agreement with the exact solution in Figure 4(a). Second, from Figures 4(c) and 4(d) it can be seen that in the case of noisy data, the retrieved solution is reasonably stable and it becomes more accurate as the amount of noise p decreases.

4.3. Example 3

We take the input data as

$$q_1(t) = -\frac{3}{4}, \quad q_2(t) = 0, \quad k(x, t) = 1, \quad S(x, t) = 0, \quad (47)$$

$$T_0(x) = 5 + \begin{cases} (x - \frac{1}{2})^3, & 0 \leq x \leq \frac{1}{2} \\ 0, & \frac{1}{2} \leq x \leq 1 \end{cases}, \quad (48)$$

$$T(x, t) = Y^{exact}(x, t) = 5 - 4t + \begin{cases} (x - \frac{1}{2})^3, & 0 \leq x \leq \frac{1}{2} \\ 0, & \frac{1}{2} \leq x \leq 1 \end{cases}. \quad (49)$$

The analytical solution of the inverse problem is given by

$$q(x, t) = \begin{cases} \frac{6x+1}{5-4t+(x-\frac{1}{2})^3}, & 0 \leq x \leq \frac{1}{2} \\ \frac{4}{5-4t}, & \frac{1}{2} \leq x \leq 1 \end{cases}. \quad (50)$$

The example has also been considered in [10] and it consists of retrieving non-smooth but continuous perfusion coefficient (50).

We take the initial guess $q^0(x, t) = 2$.

Figure 5(a) shows the monotonic decreasing convergence of the objective functional (5), as a function of the number of iterations n , for various amounts of noise $p = 0$ (no noise) and $p\% \in \{1, 2\}\%$ noisy data (37). For noisy data, the intersection of horizontal lines $y = \frac{1}{2}\mu^2(p)$, with the graphs of $J[q^n]$ yields the stopping iteration numbers $n_d(p) \in \{40, 24\}$ for $p \in \{1, 2\}$, respectively, according to the discrepancy principle (26). These values can then be compared with the optimal ones of $n_{opt}(p) \in \{34, 21\}$ for $p \in \{1, 2\}$, respectively, obtained by plotting the error curves $E(q^n) = \|q^n - q\|_{L^2(0,1)}$, as functions of the number of iterations n , in Figure 5(b). The comparison shows that n_d and n_{opt} are close to each other.

The numerical results are illustrated in Figure 6 and the same conclusions as those obtained for *Example 2* can be reported.

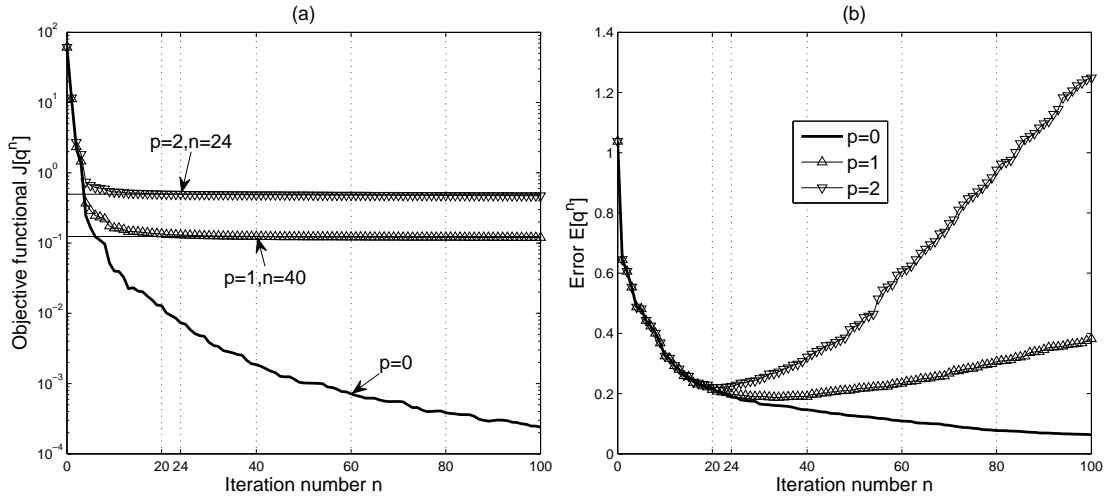


Figure 5: (a) the objective functional $J[q^n]$ and (b) the error $E[q^n]$ for $p \in \{0, 1, 2\}$, for *Example 3*.

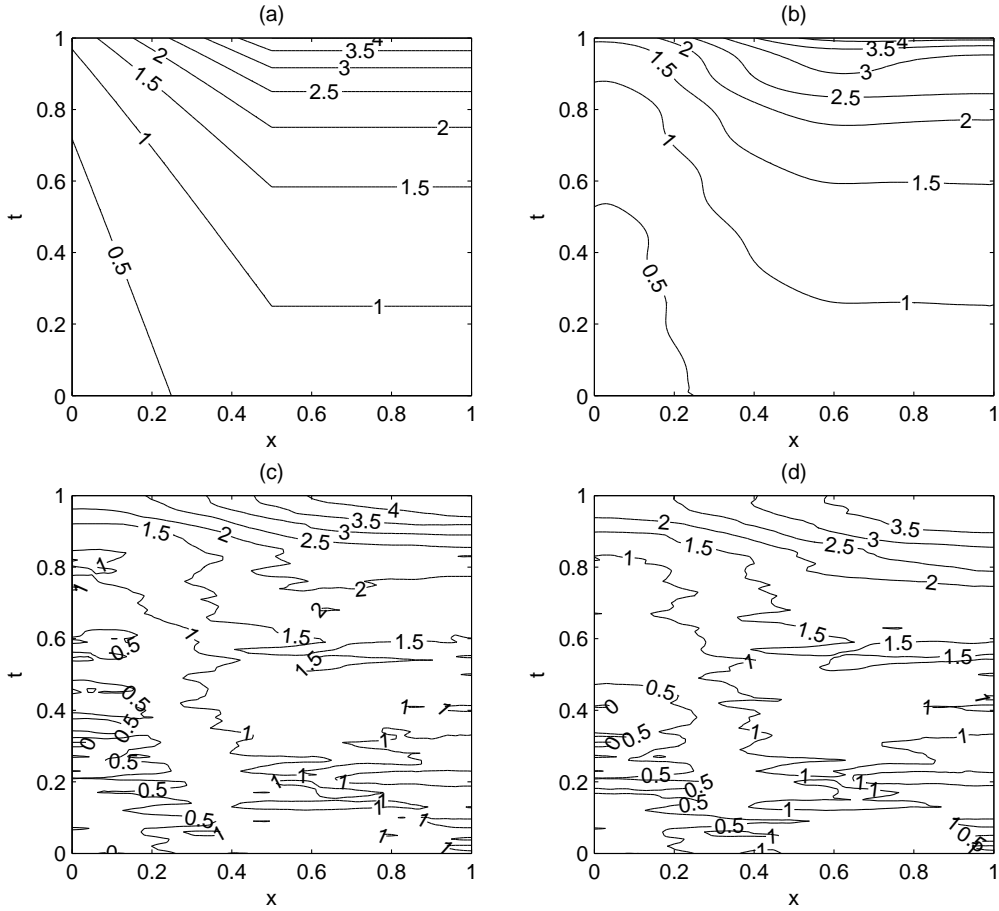


Figure 6: (a) The exact and estimated perfusion coefficient $q(x, t)$ with (b) $p = 0$, (c) $p = 1$, and (d) $p = 2$, for *Example 3*.

4.4. Example 4

Finally, we consider reconstructing a more physical example represented by a discontinuous perfusion, as it is well-known that the blood perfusion has a different value for healthy tissue than

for a tumour, [3]. We take the input data as

$$q_1(t) = 1, \quad q_2(t) = 0, \quad k(x, t) = 1, \quad S(x, t) = 0, \quad (51)$$

$$T_0(x) = 2 + \begin{cases} (x - \frac{1}{2})^2, & 0 \leq x \leq \frac{1}{2} \\ 0, & \frac{1}{2} < x \leq 1 \end{cases}, \quad (52)$$

$$T(x, t) = Y^{exact}(x, t) = 2 - t + \begin{cases} (x - \frac{1}{2})^2, & 0 \leq x \leq \frac{1}{2} \\ 0, & \frac{1}{2} < x \leq 1 \end{cases}. \quad (53)$$

Then the analytical solution of the inverse problem is given by

$$q(x, t) = \begin{cases} \frac{3}{2-t+(x-\frac{1}{2})^2}, & 0 \leq x \leq \frac{1}{2} \\ \frac{1}{2-t}, & \frac{1}{2} < x \leq 1 \end{cases}. \quad (54)$$

Remark that, unlike the previous examples, $q(x, t)$ is discontinuous on the line $x = 1/2$, $t \in [0, 1]$, hence the example (54) is more severe.

We take the initial guess $q^0(x, t) = 0.5$.

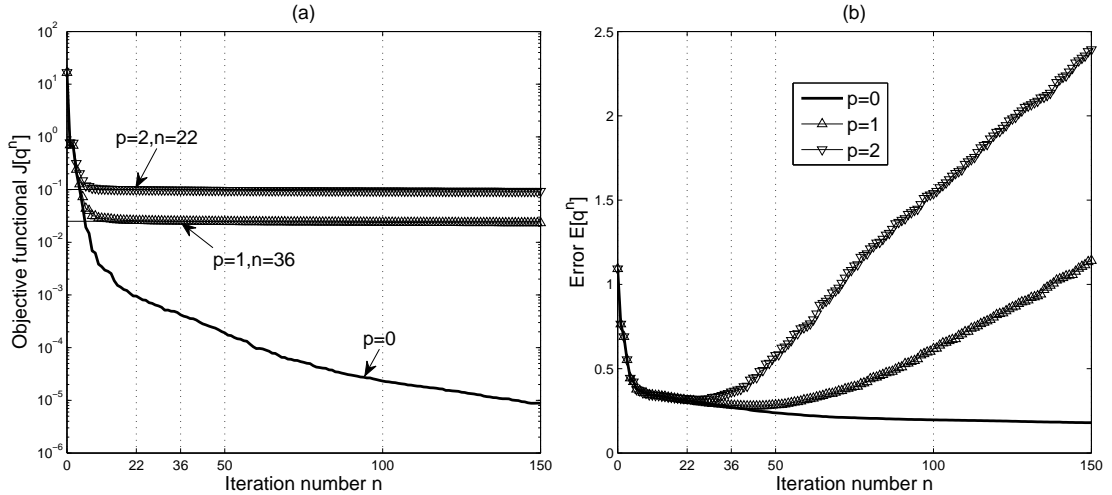


Figure 7: (a) The objective functional $J(q^n)$ and (b) the error $E(q^n)$ for $p \in \{0, 1, 2\}$, for *Example 4*.

Figure 7(a) shows the monotonic decreasing convergence of the objective functional (5), as a function of the number of iterations n , for various amounts of noise $p = 0$ (no noise) and $p\% \in \{1, 2\}\%$ noisy data (37). For noisy data, the intersection of horizontal lines $y = \frac{1}{2}\mu^2(p)$, with the graphs of $J[q^n]$ yields the stopping iteration numbers $n_d(p) \in \{36, 22\}$ for $p \in \{1, 2\}$, respectively, according to the discrepancy principle (26). These values can then be compared with the optimal ones of $n_{opt}(p) \in \{42, 26\}$ for $p \in \{1, 2\}$, respectively, obtained by plotting the error curves $E(q^n) = \|q^n - q\|_{L^2(0,1)}$, as functions of the number of iterations n , in Figure 7(b). The comparison shows that n_d and n_{opt} are close to each other.

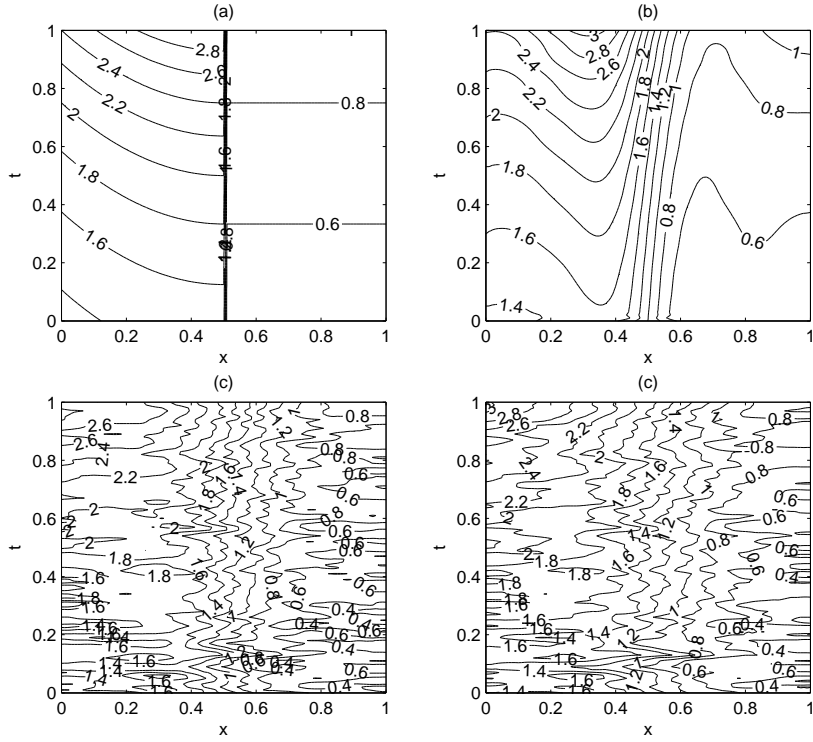


Figure 8: (a) The exact and estimated perfusion coefficient $q(x, t)$ with (b) $p = 0$, (c) $p = 1$, and (d) $p = 2$, for *Example 4*.

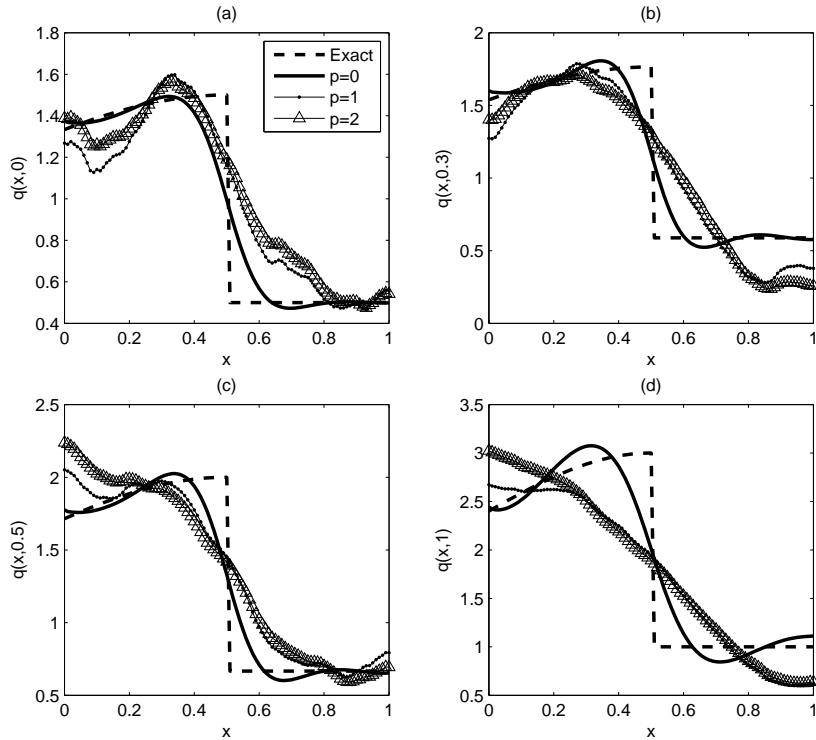


Figure 9: The exact and estimated perfusion coefficient $q(x, t)$ for $p \in \{0, 1, 2\}$ at (a) $t = 0$, (b) $t = 0.3$, (c) $t = 0.5$, and (d) $t = 1$, for *Example 4*.

The numerical results are illustrated in Figures 8 and 9. In the case of no noise in Figure

8(b), the results are plotted after 150 iterations, whilst for noisy data the results are plotted after $n_d(p)$ iterations. First, from Figures 8(b) and 9 it can be seen that in the case of no noise, the retrieved solution is in good agreement with the exact solution. From Figure 9, we can also find that the retrieved solution with no noise is in good agreement with the exact solution for $t \in [0, 1]$. Of course, the numerical results do deviate from the exact solution near the point $x = 0.5$ for $t \in [0, 1]$, since from (54) the exact perfusion coefficient $q(x, t)$ is discontinuous at $x = 0.5$. Second, from Figures 8(c), 8(d) and 9 it can be seen that in the case of noisy data, the retrieved solution is still reasonably stable and it becomes more accurate as the amount of noise p decreases.

5. Conclusions

In this paper, the determination of the space- and time-dependent perfusion coefficient from temperature measurements has been investigated using the CGM. Regularization has been achieved by stopping the iterations at the level at which the least-squares objective functional, minimizing the gap between the computed and the measured temperature, becomes just below the noise threshold with which the data is contaminated. Compared to the previous numerical methods developed in [10], the present CGM is more efficient and stable when inverting noisy data. Future work will consist in multi-dimensional reconstructions of the perfusion coefficient.

Acknowledgement

K. Cao would like to thank the University of Leeds and the China Scholarship Council for supporting his PhD studies at the University of Leeds.

References

- [1] E. P. Scott, P. Robinson, T. E. Diller, Estimation of blood perfusion using a minimally invasive blood perfusion probe, *ASME-Publications-HTD* 355 (1997) 205–212.
- [2] H. H. Pennes, Analysis of tissue and arterial blood temperatures in the resting human forearm, *Journal of Applied Physiology* 1 (2) (1948) 93–122.
- [3] J. Liu, L. S. Xu, Boundary information based diagnostics on the thermal states of biological bodies, *International Journal of Heat and Mass Transfer* 43 (16) (2000) 2827–2839.
- [4] H. Arkin, L. X. Xu, K. R. Holmes, Recent developments in modeling heat transfer in blood perfused tissues, *IEEE Transactions on Biomedical Engineering* 41 (2) (1994) 97–107.
- [5] J. Wren, M. Karlsson, D. Loyd, A hybrid equation for simulation of perfused tissue during thermal treatment, *International Journal of Hyperthermia* 17 (6) (2001) 483–498.
- [6] O. M. Alifanov, *Inverse Heat Transfer Problems*, Springer Science & Business Media, Berlin, 2012.

- [7] J. V. Beck, B. Blackwell, C. R. S. Clair Jr, *Inverse Heat Conduction: Ill-Posed Problems*, John Wiley & Sons, New York, 1985.
- [8] J. J. Zhao, J. Zhang, N. Kang, F. Yang, A two level finite difference scheme for one dimensional Pennes bioheat equation, *Applied Mathematics and Computation* 171 (1) (2005) 320–331.
- [9] W. Dai, H. Wang, P. M. Jordan, R. E. Mickens, A. Bejan, A mathematical model for skin burn injury induced by radiation heating, *International Journal of Heat and Mass Transfer* 51 (23) (2008) 5497–5510.
- [10] D. Trucu, D. B. Ingham, D. Lesnic, Reconstruction of the space- and time-dependent blood perfusion coefficient in bio-heat transfer, *Heat Transfer Engineering* 32 (9) (2011) 800–810.
- [11] M. V. Klibanov, T. R. Lucas, R. M. Frank, A fast and accurate imaging algorithm in optical/diffusion tomography, *Inverse Problems* 13 (5) (1997) 13–41.
- [12] D. Trucu, D. B. Ingham, D. Lesnic, An inverse coefficient identification problem for the bio-heat equation, *Inverse Problems in Science and Engineering* 17 (1) (2009) 65–83.
- [13] J. K. Grabski, D. Lesnic, B. T. Johansson, Identification of a time-dependent bio-heat blood perfusion coefficient, *International Communications in Heat and Mass Transfer* 75 (2016) 218–222.
- [14] D. Trucu, D. B. Ingham, D. Lesnic, Inverse space-dependent perfusion coefficient identification, *Journal of Physics: Conference Series* 135 (1) (2008) 012098.
- [15] Z.-C. Deng, J.-N. Yu, L. Yang, Optimization method for an evolutionary type inverse heat conduction problem, *Journal of Physics A: Mathematical and Theoretical* 41 (3) (2008) 035201.
- [16] Z.-C. Deng, L. Yang, J.-N. Yu, G.-W. Luo, Identifying the radiative coefficient of an evolutionary type heat conduction equation by optimization method, *Journal of Mathematical Analysis and Applications* 362 (1) (2010) 210–223.
- [17] Y. Jarny, M. N. Özisik, J. P. Bardon, A general optimization method using adjoint equation for solving multidimensional inverse heat conduction, *International Journal of Heat and Mass Transfer* 34 (11) (1991) 2911–2919.
- [18] J. W. Daniel, *The Approximate Minimization of Functionals*, Prentice-Hall Englewood Cliffs, New Jersey, 1971.
- [19] R. Fletcher, C. M. Reeves, Function minimization by conjugate gradients, *The Computer Journal* 7 (2) (1964) 149–154.
- [20] O. M. Alifanov, Solution of an inverse problem of heat conduction by iteration methods, *Journal of Engineering Physics and Thermophysics* 26 (4) (1974) 471–476.

- [21] M. N. Özisik, Heat Conduction, John Wiley & Sons, New York, 1993.
- [22] C. H. Huang, M. N. Özisik, Inverse problem of determining unknown wall heat flux in laminar flow through a parallel plate duct, Numerical Heat Transfer 21 (1) (1992) 55–70.